Cement and Concrete Composites 89 (2018) 260–271

Contents lists available at ScienceDirect

Cement and Concrete Composites

journal homepage: www.elsevier.com/locate/cemconcomp

Poly(methyl methacrylate) capsules as an alternative to the ''proof-of-concept'' glass capsules used in self-healing concrete

Maria Araújo [a, b], Sutima Chatrabhuti [c], Stijn Gurdebeke [a], Natalia Alderete [a, d], Kim Van Tittelboom [a], Jean-Marie Raquez [c], Veerle Cnudde [e], Sandra Van Vlierberghe [b], Nele De Belie [a, *], Elke Gruyaert [f]

[a] Magnel Laboratory for Concrete Research, Department of Structural Engineering, Faculty of Engineering and Architecture, Ghent University, Tech Lane Ghent Science Park, Campus A, Technologiepark Zwijnaarde 904, 9052 Ghent, Belgium
[b] Polymer Chemistry and Biomaterials Group, Centre of Macromolecular Chemistry, Department of Organic and Macromolecular Chemistry, Faculty of Sciences, Ghent University, Krijgslaan 281, Building S4-bis, 9000 Ghent, Belgium
[c] Laboratory of Polymeric and Composite Materials (LPCM), Center of Innovation and Research in Materials and Polymers (CIRMAP), Mons University, Place du Parc 23, B-7000 Mons, Belgium
[d] LEMIT, CONICET, 52 entre 121 y 122 s/n, 1900 La Plata, Argentina
[e] Centre for X-ray Tomography/PProGRess, Department Geology and Soil Science, Faculty of Sciences, Ghent University, Krijgslaan 281, S8, 9000 Ghent, Belgium
[f] Structural Mechanics and Building Materials, Technology Cluster Construction, Department of Civil Engineering, KU Leuven, Gebroeders De Smetstraat 1, 9000 Ghent, Belgium

A R T I C L E I N F O

Article history:
Received 2 January 2018
Received in revised form
21 February 2018
Accepted 25 February 2018
Available online 2 March 2018

Keywords:
Self-healing concrete
Poly(methyl methacrylate)
Cylindrical capsules
Cracks

A B S T R A C T

Development of suitable capsules is essential to achieve self-healing by encapsulation. In the context of self-healing concrete, capsules that can be easily mixed into concrete and release the healing agent when cracking occurs are ideally required. The optimization of these properties would allow for a successful implementation at large scale in practical (concrete) applications. In the present work, the suitability of polymeric cylindrical capsules made of poly(methyl methacrylate) (PMMA) to carry healing agent in self-healing concrete has been evaluated. An innovative method to assess more easily the capsules survival during concrete mixing was developed. This method is based on the evaluation of the setting behavior of concrete containing capsules filled with setting accelerator. Capsules with a wall thickness of 0.7 mm were able to resist the concrete mixing process and to rupture at relatively small crack widths (116 μm) after applying a surface treatment to increase the adhesion between the capsules and the cementitious matrix. Next, the self-healing efficiency of the encapsulation materials (glass or PMMA) was evaluated on real-scale concrete beams. The results showed that cracked concrete beams with mixed-in capsules (glass or PMMA) filled with water-repellent agent showed higher resistance against chloride ingress compared to plain cracked concrete beams. PMMA capsules showed a lower self-healing efficiency (in relation to chloride ingress) compared to glass due to a less favorable distribution of the capsules in the concrete. However, concrete containing glass capsules is susceptible towards alkali-silica reaction.

Although optimization of the PMMA capsules is still necessary to improve their distribution in concrete and achieve higher self-healing efficiency, the obtained results indicate that these capsules could be a promising solution towards self-healing concrete.

© 2018 Elsevier Ltd. All rights reserved.

1. Introduction

Polymeric healing agents have the ability to seal cracks and to bond the crack faces together. Up to now, most healing agents are supplied to the cracks using spherical [1–8] or cylindrical capsules [9–14], hollow fibers [15,16] or vascular systems [17,18]. In an encapsulation-based self-healing system, the capsules are randomly dispersed within the matrix so when cracks develop, some of these capsules are crossed by the crack resulting in rupture and subsequent release of the healing agent into the crack through

* Corresponding author.
E-mail address: nele.debelie@ugent.be (N. De Belie).

https://doi.org/10.1016/j.cemconcomp.2018.02.015
0958-9465/© 2018 Elsevier Ltd. All rights reserved.

capillary action. Certain criteria such as protection of the healing agent for a long time (up to several years) and the ability to release the content upon crack formation should be met by the capsule material. Moreover, capsules that can resist the concrete mixing process (i.e. high impact of the mixer and aggregates on the capsules and high shear stress exposure) are highly desired. As a result, the concrete production process would not be too much affected and the processing cost would not increase. Hence, self-healing concrete could effectively become valorized and interesting towards industrial application.

Most research has mainly focused on the development of organic spherical microcapsules or the use of cylindrical capsules (e.g. glass) to encapsulate the healing agent. Urea-formaldehyde (UF), gelatin, silica, melamine-urea-formaldehyde (MUF), phenol-formaldehyde (PF) and polyurethane (PU) microcapsules have been often used to encapsulate different healing agents in order to realize self-healing of cementitious materials [4–7,19,20]. Typically for spherical capsules the capsule diameters reported in literature range from 5 μm to 5 mm. One of the main concerns with the use of spherical microcapsules in concrete is that they can only sequester a very limited amount of healing agent and therefore become rapidly exhausted with increasing crack width. On the contrary, large crack volumes can be healed with cylindrical capsules and their fracture probability upon concrete cracking is possibly higher. However, it is less probable that they would resist the mixing forces during mixing of concrete [21]. While some authors proposed to increase the probability to survive casting and mixing of brittle capsules (i.e. glass and ceramic) by applying a cement paste coating [22], others have attempted to develop polymeric capsules with switchable mechanical properties so they can resist the mixing forces and break upon crack formation [9,10]. Due to their inertness to the healing agent and brittle nature (i.e. can be ruptured easily), hollow glass tubes have mostly been used for proof-of-concept experiments to investigate the self-healing efficiency of liquid healing agents [11–14,23]. Most of the glass capsules used up to now would probably not resist the concrete mixing process without protection. Therefore, these glass capillaries are typically carefully placed inside mortar or concrete. More recently, Feiteira [24] showed that thicker glass capsules (0.80–1.5 mm) can resist the concrete mixing process. However, one main concern with the use of glass capsules in concrete is that they might induce alkali-silica reactions (ASR) if a high amount of alkali is present in the cementitious matrix. Polymeric tubular capsules can be an alternative to the glass capsules as they are likely easier (and cheap) to manufacture in larger quantities. Moreover, polymeric materials can be found and designed with a wide range of mechanical properties which could possibly facilitate to develop capsules that can fulfill the two contradictory requirements: brittleness for rupturing when a crack forms and high flexibility and impact resistance to have a good survival probability when mixed with concrete. Hilloulin et al. [10] used polymeric materials which were brittle at room temperature and characterized by a relatively low glass transition temperature (i.e. T_g between 59 and 105 °C) to prepare hollow tubes. By heating (above T_g) the tubes beforehand, their survival probability during concrete mixing was increased. Gruyaert et al. [9] mixed various plasticizers with ethyl cellulose to extrude tubes with evolving brittleness due to leaching of the plasticizer. The capsules could easily survive the concrete mixing process but breakage upon crack formation was not achieved. Though some advances have been achieved during the development of encapsulation materials to obtain autonomous healing of cracks in cementitious materials, suitable and appropriate capsules for polymeric healing agents which can be applicable in practice have not yet been identified to date. The present work covers an investigation on the suitability of poly(methyl methacrylate) (PMMA) as an alternative to frequently used glass for capsules to apply at a large scale in practical concrete structures. The selection of poly(methyl methacrylate) was based on its ability to rupture when crossed by small cracks (100 μm) as demonstrated previously [25]. In this study, PMMA capsules with varying dimensions were obtained by extrusion and optimized to be able to resist to the concrete mixing process and at the same time break when intersected by cracks. An innovative method to assess more easily the capsules survival rate during concrete mixing is also presented. The self-sealing/healing of the best suited PMMA capsules was then evaluated in large concrete elements. Since one of the main limitations of these capsules is still their incapability of keeping air/moisture curing healing agents from premature hardening before release and healing takes place, a water repellent agent was selected to be used in combination with these capsules to regain the impermeability of cracked concrete.

2. Materials and methods

2.1. Capsule design for self-healing concrete

2.1.1. Extrusion of the PMMA capsules

PMMA (Plexiglas 8909, $M_n = 38000$ g/mol), used to extrude the hollow tubes, was supplied by Evonik Performance Materials (Darmstadt, Germany).

To avoid hydrolysis, PMMA was dried under vacuum during 24 h at 60 °C before extrusion. A laboratory-scale Brabender single screw extruder, equipped with a die with outer and inner diameter respectively of 10 mm and 8 mm, was used to obtain the PMMA hollow tubes.

The processing temperature and parameters used during the extrusion process are shown in Table 1. Capsules with varying wall thickness were prepared by adjusting the conveyor speed.

The glass capsules used as reference materials had an external diameter of 5.0 mm and a wall thickness of 0.8 mm and were obtained from Glasatelier Saillart BVBA (Meerhout, Belgium).

2.1.2. Capsule survival probability with respect to concrete mixing process

First, the survival probability of capsules in self-healing concrete produced at laboratory scale was assessed by the previously described method of manual counting after concrete mixing [9,10]. Mixed-in capsules were inspected on their completeness after removal of the cement paste by sieving. This facilitates the manual retrieval and counting of the intact capsules. The survival probability was then calculated by relating the number of intact capsules to the original number of capsules added to the concrete mix.

Different parameters influencing the survival rate of capsules were studied:

i. capsule material (PMMA vs. glass);
ii. capsule dimensions (i.e. wall thickness);
iii. concrete composition (traditional concrete (TC) with crushed aggregates vs. self-compacting concrete (SCC) with rounded aggregates (Table 2) and;
iv. concrete mixer (Creteangle forced action pan mixer (type SE/GB) with a maximum capacity of ~14 l vs. Eirich vertical shaft mixer with rotating pan and maximum capacity of 50 l).

The same mixing procedure was used throughout the study and consisted of mixing the dry components during 1 min, followed by addition of the water and mixing for another minute. Subsequently, the capsules were added and all components were mixed during two additional minutes.

Since the method relying on counting the intact capsules is

Table 1
Extrusion parameters and dimensions of the PMMA capsules.

Processing temperature (°C)	Screw speed (min^{-1})	Torque (Nm)	Die pressure (bar)
235–225	10	103	18.8
Conveyor speed (m/min)	Capsule dimensions External diameter (mm)	Wall thickness (mm)	Length (mm)
0.5	6.5 ± 0.3	0.7 ± 0.1	50
1.0	5.9 ± 0.6	0.4 ± 0.1	50
1.2	5.8 ± 0.3	0.2 ± 0.1	50

Table 2
Concrete compositions used for the mixing tests.

Traditional concrete (1 m^3)	
Components	(kg)
Sand 0/5	664
Crushed stones 2/6	450
Crushed stones 6/20	760
CEM I 52.5 N	350
Water	165
Self-compacting concrete (1 m^3)	
Components	(kg)
Sand 0/5	853
Gravel 2/8	370
Gravel 8/16	328
Limestone filler	300
CEM I 52.5 N	300
Water	165
Superplasticizer (Glenium 51)	2.5 (l)

time-consuming and not practically applicable for larger concrete mixes containing hundreds of capsules, alternative methods were investigated, based on the evaluation of the setting behavior of concrete containing capsules filled with set accelerator. If the effect of a given amount of set accelerator on certain concrete properties is known, measuring of those concrete properties allows to back-calculate the amount of set accelerator in the mix and hence the amount of capsules that have been broken.

Therefore, first a calibration curve showing the influence of the amount of set accelerator on the setting time of concrete was formulated. Then, concrete mixes containing different amounts (0, 0.25, 0.5, 1, 1.2 and 1.5 wt% vs. cement weight) of set accelerator (SIKA FS1) were produced. The setting was monitored by performing (i) penetrometer tests and (ii) ultrasonic (US) P-wave transmission measurements. The mixing procedure used was the same as described previously, however, in these tests a self-compacting concrete (SCC) mix was used since the fresh concrete had to be sieved to perform the penetrometer tests and this is more convenient for SCC mixes than for traditional concrete mixes with a water-to-cement ratio of 0.5 and without plasticizers. The SCC mix composition used is shown in Table 2.

The penetrometer tests were performed using the procedure described in the standard ASTM C403, but the concrete was sieved on a 4 mm sieve instead of a 4.75 mm sieve as prescribed by ASTM C403 in order to eliminate the coarse aggregates and capsules. Initial and final setting times were determined at a penetration resistance value of respectively 3.5 and 27.6 MPa.

The FreshCon system developed at the University of Stuttgart [26] was used to perform the US measurements. The parameter studied was the P-wave velocity, determined based on the detection of the onset time of the signal with the AIC picking algorithm taking into account the time delay due to the travel of the pulse through hardware, sensors and container walls. Penetrometer tests and continuous US measurements were executed in a climate room at a temperature of 20 °C and a relative humidity of 60%.

Next, SCC mixes containing encapsulated set accelerator (1 wt% vs. cement weight) were produced and the setting behavior was monitored. This 1 wt% amount corresponded to the total amount of accelerator contained by all the capsules. The number of capsules added varied slightly depending on the capsule type, since the amount of set accelerator that can be stored inside one single capsule depends on its internal diameter.

Based on the calibration curve, the amount of set accelerator released (due to damage of the capsules) was determined, giving an indication of the number of capsules which had survived the mixing process. Moreover, a part of the concrete mixes (~10 l) was inspected manually to additionally assess the survival probability by the method relying on counting the number of intact capsules after mixing.

The mix composition (except the accelerator or capsule content), mix procedure, test conditions (e.g. temperature) and testing procedures were kept constant during the calibration and the effective tests.

2.1.3. *Capsule breakage upon crack formation*

In a previous study [25], it was shown that the PMMA capsules could be broken when intersected by a crack. However, in the same study, to ensure that the capsules would not slip during crack formation, the ends of the capsules were heated and bent to create hooks. In addition, the capsules were sanded perpendicular to their length to improve the bond with the cementitious matrix. As the hooked ends could create additional weak points of breakage during concrete mixing and the latter is very difficult and time-consuming to implement in reality, in the present work, the rupture capability upon crack formation has been evaluated, of PMMA capsules that were either non-treated or treated by use of alternative strategies compatible with translation to actual, real-life applications. Five different treatments were considered as indicated in Fig. 1: (A) the capsules were sanded perpendicular to their length to create a rough surface and to increase the bond to the matrix; (B) a sand layer was applied to both ends of the capsules to anchor the capsules and avoid slippage; (C) a coarse surface was created by applying a sand layer at one side of the capsule to increase adhesion and to prevent capsules from becoming pulled out from the matrix; (D) a combination of treatments A and C to further improve the adhesion to matrix and; (E) a combination of treatments A and B.

Since capsules with a wall thickness of 0.2 and 0.4 mm could not survive the concrete mixing process (section 3.1), only capsules with a wall thickness of 0.7 mm were selected for further testing.

To determine the crack width at breakage, mortar specimens with dimensions of 40 mm × 40 mm × 160 mm containing one single capsule, positioned in the middle of the specimen at approximately 1.3 cm from the bottom, were casted.

Based on the results of the survival tests, only capsules with a wall thickness of 0.7 mm (outer diameter = 6.5 mm,

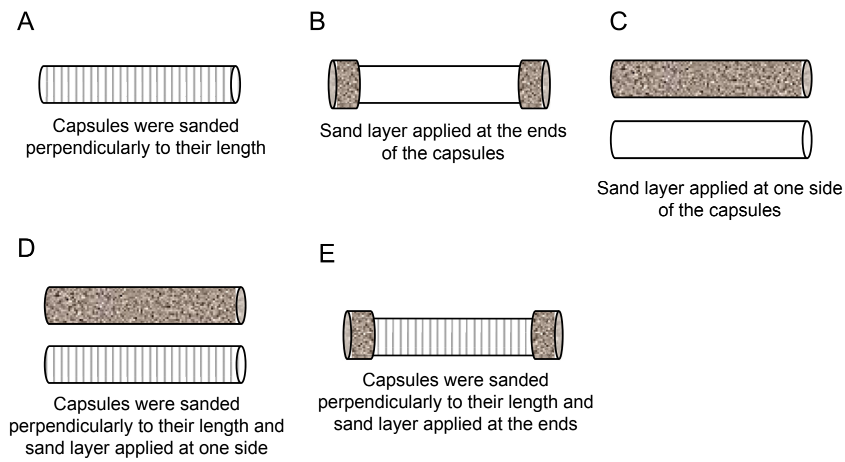

Fig. 1. Various surface treatments applied onto the PMMA capsules.

length = 50 mm) were chosen for testing. The capsules were filled with water and sealed with hot glue at the ends. The mortar mix consisted of CEM I 52.5N with a water-to-cement ratio of 0.5 and a sand-to-cement ratio of 3 and were prepared according to the European Standard EN 196-1.

Cracking of the mortar prisms was performed at the age of 14 days by loading the samples in a three-point-bending test. A linear variable differential transformer (LVDT) positioned at the bottom side of the specimen as described in Ref. [25] was used to measure the crack width. The crack width was increased at a speed of 1 μm s^{-1} up to 400 μm.

2.1.4. Release of healing agent upon crack formation

The ability of the PMMA capsules (wall thickness = 0.7 mm, outer diameter = 6.5 mm, length = 50 mm) to release their content upon crack formation was evaluated via a capillary water absorption test by determining the regain in impermeability of cracked samples. The PMMA capsules were sanded in the direction perpendicular to their length as described before. Glass capsules (wall thickness = 0.8 mm, outer diameter = 5.0 mm, length = 50 mm) were also considered as reference materials.

The capsules were filled with a water-repellent agent (which renders the crack faces impermeable) and embedded in mortar. Each mortar specimen contained one capsule, positioned in the middle plane and at a height of 1.3 cm, and was prepared according to the procedure described in the previous section.

At the age of 14 days, the mortar specimens were cracked via a crack width controlled 3-point-bending test (as described in section 2.1.3). The crack width was increased at a speed of 1 μm s^{-1}; until a width of 250 μm was obtained. The capillary water absorption test was performed 2 days after cracking.

The capillary water absorption measurements were conducted as described earlier [27]. The sorption coefficients were determined from the slope of the curves obtained by plotting the water uptake as a function of the square root of time, according to the European Standard EN 13057.

2.2. Capsule performance in a large-scale lab test

2.2.1. Concrete beams with(-out) capsules

To validate the self-sealing efficiency of the capsules in large concrete elements, three real-scale concrete beams (250 cm × 40 cm × 20 cm) reinforced with 4 Ø 10 mm ribbed steel bars were made. Two of them contained self-sealing properties provided by either PMMA (wall thickness = 0.7 mm, outer diameter = 6.5 mm, length = 50 mm) or glass capsules (wall thickness = 0.8 mm, outer diameter = 5.0 mm, length = 50 mm). The capsules were sealed at one end with hot glue (PMMA) or epoxy resin (glass), filled by means of a needle with a water-repellent agent and sealed again at the other end. Moreover, the PMMA capsules were sanded in a direction perpendicular to their length (as aforementioned).

The third beam was a reference beam without capsules. The concrete mixes consisted of self-compacting concrete (Table 2) and were prepared using a vertical shaft mixer with a maximum capacity of 200 L. The concrete composition was the same for all the mixes but for the concrete beams with self-healing properties, PMMA or glass capsules were added in the last 2 min of the mixing process. Since it was observed that PMMA capsules tend to float as a result of their relatively low density, it was decided to cast the concrete in 2 steps. First, a concrete mix containing the capsules with a concentration of approximately 22 capsules per liter of concrete (3250 capsules in 150 l concrete) was made and poured into the mould, forming a layer of 12 cm. Afterwards, another mix without capsules was prepared and placed into the mould on top of the previous layer. Although, the glass capsules do not tend to float, the beam containing these capsules was cast in the same manner in order to have the same conditions.

After demoulding, the beams were stored in a standard laboratory environment until the time of testing.

2.2.2. Crack formation

At the age of 14 days, 6 cracks with varying crack widths were made in each beam using a 3-point-bending test set-up. The cracks were created consecutively (one crack per day) by moving the 3-point-bending set-up over the length of the beam (Fig. 2). Notches were swan at the corners of the beam in the middle of the span of the 3-point-bending set-up prior to loading. Localized cracks were then created by loading the beams in a stepwise fashion while the crack width was measured using an electronic ruler. When a predefined crack width was reached (Table 3), the notches were filled with a shrink-free repair mortar in order to keep the crack open. The beams were then unloaded after sufficient hardening of the repair mortar. The crack widths obtained after unloading for each beam were determined afterwards using an optical microscope. For each crack, crack width measurements were performed at 6 positions (at the crack mouth) over the length of the crack.

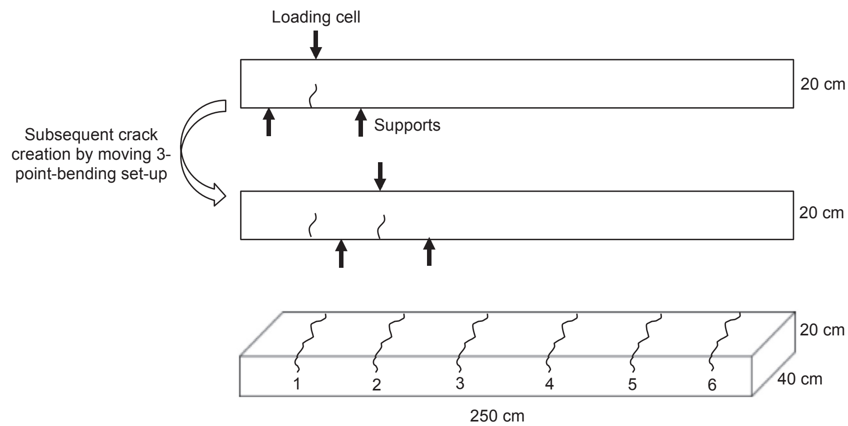

Fig. 2. Schematic representation of the test set-up of the 3-point bending test.

Table 3
Max crack width at loading for each concrete beam.

Crack	Predefined width (mm)	Max crack width at loading (mm)		
		REF	PMMA	Glass
1	0.40	0.42	0.42	0.42
2	0.60	0.53	0.55	0.54
3	0.35	0.36	0.36	0.39
4	0.50	0.48	0.49	0.48
5	0.60	0.61	0.61	0.67
6	0.45	0.44	0.44	0.45

2.2.3. Chloride ingress measurements

The self-healing efficiency of the concrete beams with embedded capsules was evaluated by determining the resistance of the self-healed concrete against chloride ingress. To this, the beams were positioned slightly tilted with the cracks in the upper surface and a 3 wt% NaCl solution was flown over the beams during 24 uninterrupted hours per week. This 1 day wet – 6 days dry cycle was repeated during 6 consecutive weeks. Prior to exposure, all sides of the beams except the top and bottom surfaces were covered with a waterproof aluminum foil so that only the top surface was exposed to the chloride solution.

To determine the chloride ingress, 2 cores with a diameter of 150 mm, with a crack inside, were obtained from each beam. Subsequently, each core was split along the crack surface and one half was then used to measure the chloride ingress. This was done by grinding off material at various depths (5, 25, 50 and 85 mm) in 2 mm layers perpendicular to the crack face. In addition, material was ground from the exposed surface downwards. Concrete powders were collected from ten layers for each zone and dried in an oven at 95 °C for at least 7 days. A schematic representation of the ground surfaces is given in Fig. 3. As can be seen, for each core, the position of the ground areas on the crack face varies slightly. This is due to the fact that for some of the cores an irregular crack face was obtained after splitting and a relatively flat area had to be chosen in order to be able to grind off material.

The total chloride concentration per ground layer was determined by an acid-soluble extraction in a nitric acid solution followed by a potentiometric titration against silver nitrate [28].

2.2.4. Capsule distribution (by X-ray micro-tomography)

After testing, multiple cores were drilled from the beams for further analysis. One core (with a diameter of 150 mm) of each beam containing glass or PMMA capsules was scanned at the Center for X-ray Tomography of Ghent University (UGCT) using the X-ray micro-tomography (μCT) [29] cone beam set-up of the High-Energy CT system Optimized for Research (HECTOR) scanner [30]. For each scan, 913 projections were acquired over an angle of 360°. To reduce beam hardening, low energetic X-rays at the source were blocked using a cupper filter of 0.5 mm thickness. The X-ray tube provided a voltage of 200 kV with a power of 30 W. The source-detector distance was 1047 mm and the source-object distance was 373 mm, resulting in a voxel size of 140 μm. The in-house developed software [31,32] was used to reconstruct the raw data into cross-sectional images (slices). These images were then used to generate a 3D rendering (using VGStudioMax) of the specimens which could be used to assess the distribution of the capsules in the concrete cores and possible leakage of healing agent from the capsules.

2.2.5. Oberholster test

The resistance of the concrete containing glass capsules to the alkali-silica reaction (ASR) was determined using the accelerated Oberholster test method. Six cylinders (age: ~6 months) with a diameter of 50 mm and approximately 160 mm height were taken from the beam containing glass capsules and placed in the measurement set-up. One steel reference sample was also placed inside the container in order to exclude expansions due to external factors (e.g. temperature variations). The dial gauges were then installed on top of the samples and the container was filled with water. The water was heated up to 80 °C and the cylinders were kept in the water for 24 h. Afterwards, the water was replaced by a 1M NaOH solution and a reference measurement was taken 1 h after the temperature of this solution had been stabilized at 80 °C. The expansion of the test and reference specimens was measured for a period of 14 days.

3. Results and discussion

3.1. Survival probability to the concrete mixing process

Fig. 4A presents the calibration curves based on the penetrometer tests performed on mixes containing a known amount of set accelerator. As can be clearly seen, the initial and final setting times decrease with increasing dosage of set accelerator in the mix. A linear relationship between the initial/final setting time and set accelerator content could be drawn as given by equations (1) and (2), respectively. While the r^2-values are still acceptable (0.75–0.83), the repeatability, as observed for the reference mix without set accelerator, is limited. Although, the penetrometer test conditions (i.e. temperature during the test) were kept constant,

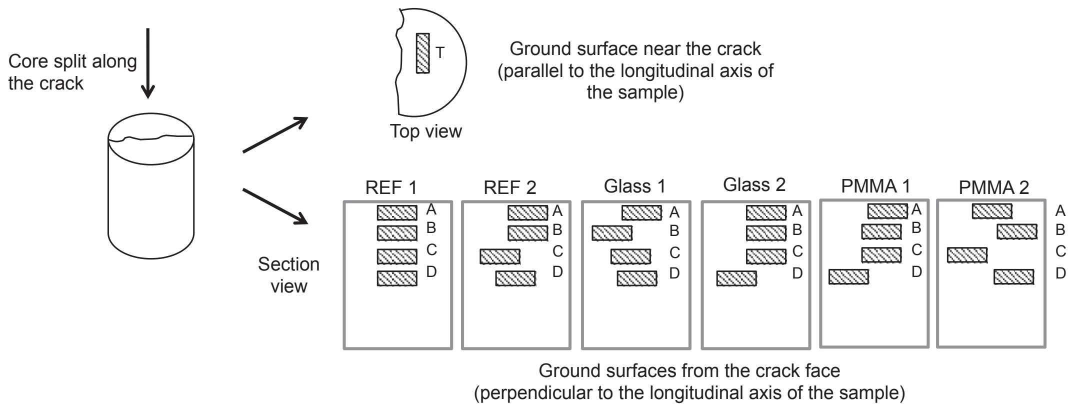

Fig. 3. Grinding method to collect powder for potentiometric titrations.

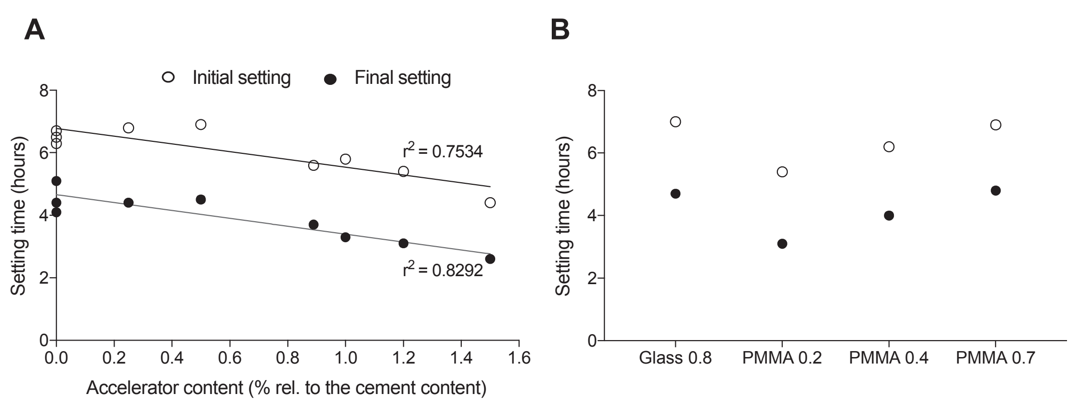

Fig. 4. Calibration curve showing the influence of the accelerator dosage on the initial and final setting time of SCC concrete (A); Initial and final setting time for SCC mixes containing different types of capsules with 1 m% accelerator (B). Glass 0.8 = glass capsules wall thickness 0.8 mm; PMMA 0.2, 0.4 and 0.7 = PMMA capsules wall thickness 0.2, 0.4 and 0.7 mm, respectively.

the concrete raw components were not acclimatized and concrete mixing did not take place in a temperature and humidity controlled room. A variation in temperature during concrete mixing of about 5 °C was monitored, which could explain the variation obtained for the reference mixtures. In future tests, this aspect should be taken into account.

$$\textit{Initial setting time}\,[hours] = -1.265 \times \textit{accelerator content}\,[wt.\%] + 4.66 \quad (1)$$

$$\textit{Final setting time}\,[hours] = -1.243 \times \textit{accelerator content}\,[wt.\%] + 6.782 \quad (2)$$

Fig. 4B presents the setting time obtained for the mixes containing the various capsules filled with 1 wt% of set accelerator. Taking into account the initial content of 1 wt%, the survival ratio for the different types of capsules in the SCC mixes could be determined. The results are presented in Table 4 and discussed in the sections below.

The UPV calibration curves are shown in Fig. 5A. The acceleration of the setting behavior for mixes with increasing dosages of the set accelerator is clearly visible. The dormant period decreases and UPV-values at early age increase by the addition of set accelerator as also reported by Ref. [33]. As can be seen in Fig. 5B, exact determination of the capsule's survival ratio is quite difficult based on the graphs solely. A rough estimate of the survival ratio for each of the PMMA capsules is given in Table 4.

Table 4 summarizes the results on survival of glass and PMMA capsules in concrete, determined by counting manually the number of intact capsules after mixing, and the alternative novel methods (i.e. based on released amount of set accelerator as estimated from penetrometer and US measurements).

Capsule dimensions have a clear effect on the survival probability. As anticipated, the survival probability of the PMMA capsules increases as the wall thickness of the capsules increases. This is also expected for glass capsules as reported by Ref. [24]. These results indicate that thicker capsules can be more easily incorporated into concrete. However, this might lead to a lower self-sealing efficiency as the rupture probability upon cracking of thicker capsules will become lower. Moreover, less healing agent can be sequestered in one capsule. Furthermore, the results in Table 4 show the remarkable influence of the concrete composition and mixing equipment on the resistance of the capsules towards the mixing process. The mixing forces using an Eirich vertical shaft mixer appear to be less aggressive as considerably more capsules survived the mixing process when this mixer was used. This was particularly noticeable for PMMA capsules with a wall thickness of 0.7 mm, with the survival ratio increasing from 40 to 87%.

The stresses induced on the capsules are also lower for a SCC than for a TC mix and this is clearly reflected in the survival percentages of the glass capsules and PMMA capsules with a wall thickness of 0.2 mm and 0.4 mm.

Table 4
Survival ratio (%) of the various types of capsules for the different methods used to determine the probability of survival during mixing.

	Test parameters				Survival ratio (%)			
	Concrete	Mixer	Volume (liter)	Method	Glass t = 0.8	PMMA t = 0.2	PMMA t = 0.4	PMMA t = 0.7
Manual counting	TC	a	10	Manual counting	50	0	20	40
	TC	b	30	Manual counting	70 [24]	0	20	87
Innovative methods	SCC	b	50	Manual counting	100	20	83	95
	SCC	b	50	PM-initial set	100	0	40	100
	SCC	b	50	PM-initial set	100	0	50	100
	SCC	b	50	US	ND	0	0	75

t = wall thickness in mm; PM = penetrometer; US = ultrasonic measurement (FreshCon).
a = Creteangle forced action pan mixer (type SE/GB); b = Eirich vertical shaft mixer with rotating pan.
ND = not determined.

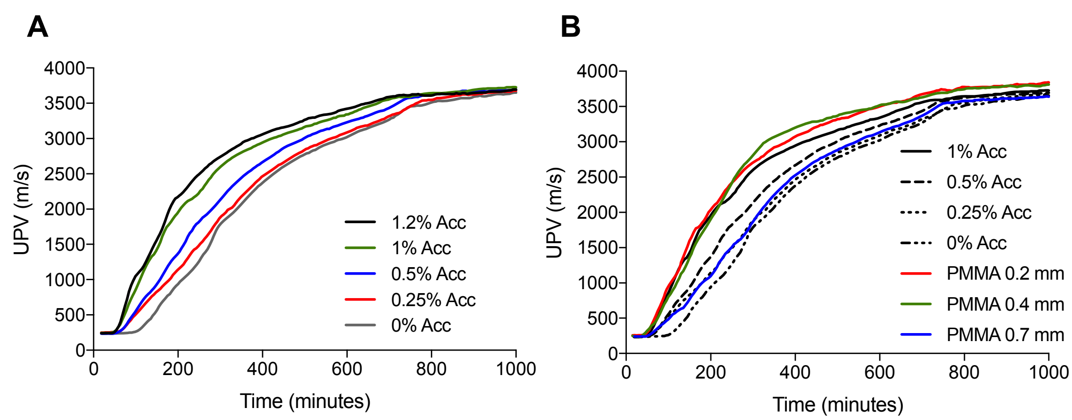

Fig. 5. Calibration curve showing the influence of the accelerator dosage on the evolution of the ultrasonic P-wave velocity (UPV) of SCC concrete (A); UPV for SCC mixes containing different types of capsules with 1 m% accelerator (B).

The alternative novel methods have been validated with the method of counting the intact capsules after concrete mixing. In general a good correspondence, except for PMMA capsules with a wall thickness of 0.4 mm, was obtained. However, the use of the penetrometer seems at the moment the most promising technique. The penetrometer test is simple to execute and analyse and the method is user-friendly. With regard to the US measurement, the test method should be further optimized and the use of retarders or air-entrainers instead of set accelerators should be evaluated.

3.2. Crack width at breakage

Since capsules with a wall thickness of 0.2 and 0.4 mm showed a low resistance towards mixing in concrete, only capsules with a wall thickness of 0.7 mm were selected for further testing. Typically, rupture of the capsules is visualized in the load-displacement graph obtained during mechanical testing (characterized by a sharp drop in the load) (Fig. 6) and is sometimes associated with a characteristic sound. This drop in load was used to determine the crack width at rupture of the capsules.

Fig. 7 shows the crack width at rupture for the different treatments applied. Smooth, non-treated capsules did not break when cracks with a width of 400 μm were created. This can be attributed to a poor adhesion of the smooth capsules to the cementitious matrix, which causes the capsules to slip. When comparing the different surface treatments, capsules that were sanded perpendicularly to their length (treatments A) ruptured at smaller crack widths (117 μm).

Applying a sand layer to both ends of the capsules did not seem to improve the locking of the capsules inside the mortar as 2 out of 3 capsules did not break during the test. Additionally, a partial

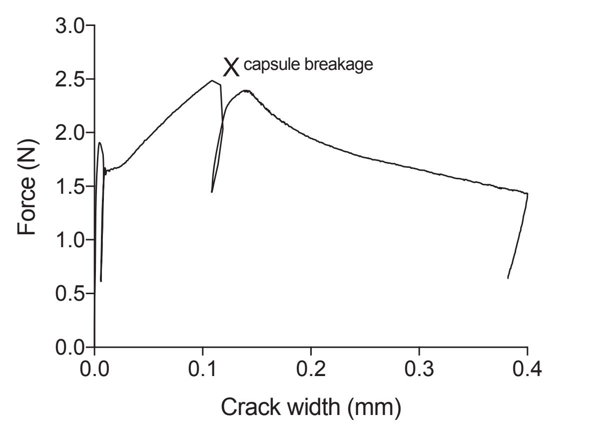

Fig. 6. Example of load drop due to rupture of the capsule during the three-point-bending test.

coating of the capsules with sand (treatment C) resulted in rupture of the capsules at a crack width of about 240 μm, which is considerably above the expected crack size at breakage (100–150 μm) as reported by Šavija et al. [25]. Capsules which were surface-treated with procedure D or E ruptured when crossed by an average crack width of 180 and 210 μm, respectively.

The results show that it is necessary to apply a surface treatment to the PMMA capsules in order to induce rupture at crack sizes typically permitted by the reinforced concrete design codes (~300 μm). Sanding the capsules (most practically feasible method) in a direction perpendicular to their length was sufficient to achieve proper adhesion between the capsule and the cementitious matrix,

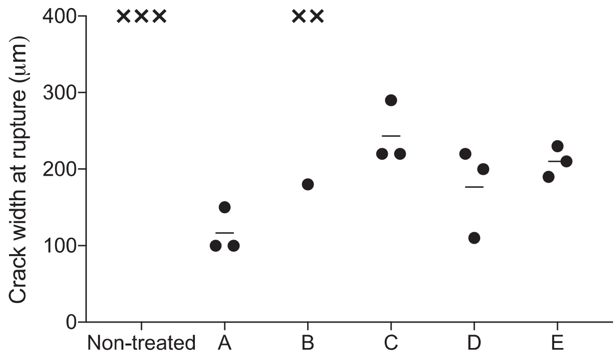

Fig. 7. Crack width at breakage of the PMMA capsules as a function of different surface treatments (●), no rupture before a crack width reaches 400 µm (x), mean value (–).

resulting in rupture of the capsules for similar crack sizes compared to those previously verified for capsules with the same wall thickness (with hooked ends) [25].

3.3. *Healing efficiency upon crack formation*

The sealing efficiency of the PMMA capsules after fracture was evaluated by means of a capillary water absorption test. The mean water sorption as a function of the square root of time and the absorption coefficients of each test series are shown in Fig. 8. The crack size (at the mouth) of the tested specimens ranged between 230 and 270 µm. The results of the capillary water absorption tests on mortar prisms containing capsules filled with water-repellent agent (WRA) clearly showed that a lower water uptake was realized for the self-healed cracked samples. No significant differences were observed between the efficiency of glass and PMMA capsules. These results show that WRA can be used in combination with PMMA capsules to regain the impermeability of cracked concrete. Since premature curing of one-component air/moisture sensitive curable healing agents may occur when using polymeric capsules as observed earlier by Hilloulin et al. [10] and Thao et al. [34], WRA can be used as an alternative to these healing agents to reduce ingress of aggressive liquids.

3.4. *Efficiency of the capsules in large concrete elements*

3.4.1. *Behavior upon crack formation*

The main aim of this study was to investigate whether polymeric (PMMA) cylindrical capsules could be used to obtain concrete with self-healing properties. The capsules should be able to survive the concrete mixing process and release their content upon intersection by a crack. Since PMMA capsules with a wall thickness of approximately 0.7 mm (outer diameter = 6.5 mm) fulfilled these 2 requirements, the self-healing efficiency of these capsules on large concrete elements was further investigated. Furthermore, glass capsules (wall thickness = 0.8 mm, outer diameter = 5 mm) were also tested and considered as reference capsules.

In order to be able to compare the crack sealing efficiency of both encapsulation materials, cracks with similar width were aimed for. The average crack widths at the crack mouth obtained after unloading of each beam are shown in Fig. 9. It can be seen that cracks with similar widths were obtained for the REF, PMMA and glass beams, except for crack 5 where a slightly higher crack width was observed for the REF beam.

It should also be mentioned that during loading of the beams containing encapsulated healing agent, leaking of the healing agent was detected, indicating that some capsules were crossed by the crack and broke. The latter was more noticeable for the beam with glass capsules with leaching out of WRA visible for all cracks. Given the brittle nature of glass (i.e. low elongation at break) compared to PMMA, glass capsules have likely more probability to be broken when crossed by a crack in concrete. The glass capsules are expected to rupture when crossed by cracks of 30 µm width [24] which is well below the crack widths at which PMMA capsules can be broken.

3.4.2. *Capsule distribution*

High-resolution X-ray computed tomography (µCT) was used to

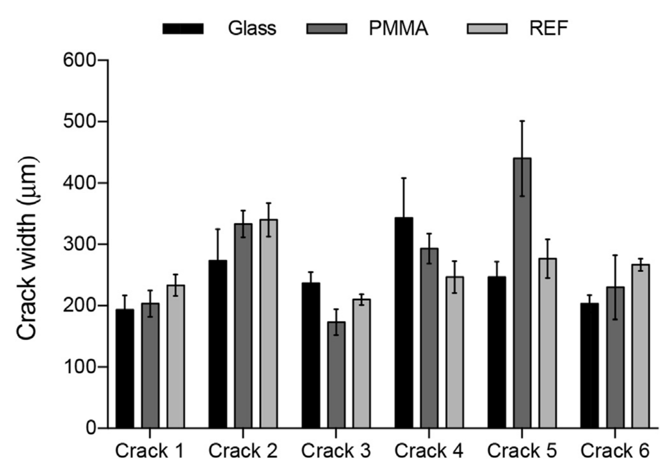

Fig. 9. Average crack width measured at the crack mouth for each beam.

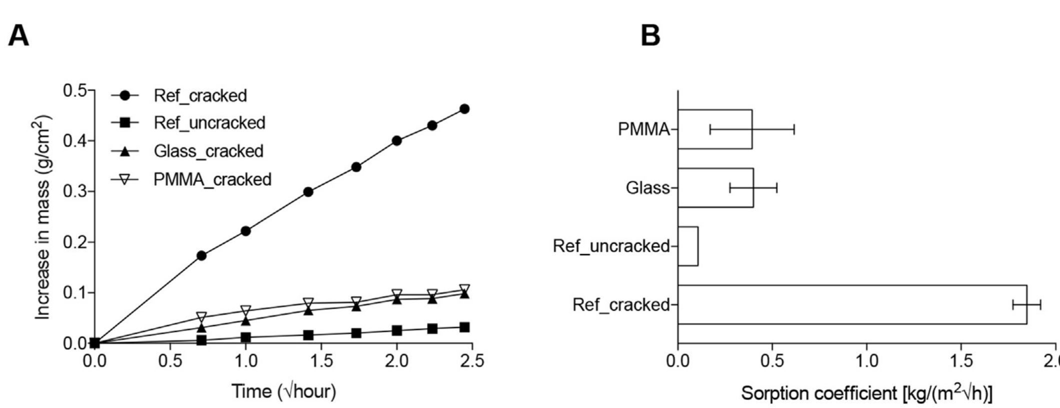

Fig. 8. Mean water absorption as a function of the square root of time (A) and the sorption coefficient (B) for each of the series. Error bars represent the standard error (n = 2–3).

characterize the distribution of the capsules in the self-healing concrete elements and leakage of WRA from the capsules after fracture of the concrete.

Scanning concrete elements with a diameter of 150 mm is very close to the limit of the HECTOR scanner capacity. Therefore, the resolution of the reconstructed images is limited.

Fig. 10A illustrates a horizontal slice through a concrete cylinder where an emptied capsule could be clearly identified. The capsules and the crack could be distinguished by selecting appropriate thresholds in OctopusAnalysis, after which a 3D rendering of the different cores was made. Since the crack is only represented by a few voxels within the reconstructed images, it was impossible to visualize it correctly in the 3D rendering. Moreover, as the healing agent (WRA) used in the large-scale experiments was absorbed by the concrete, crack filling with this fluid was undetectable on the μCT scans because of the limited resolution. The capsules were classified as empty or filled with healing agent based on the different grey levels of its contents observed on the μCT images. As air has a very low attenuation coefficient for X-rays compared to the surrounding concrete, it appears black on the reconstructed images. A capsule that has a black color is possibly filled with air instead of healing products and was classified as empty. On the contrary, in the capsules that were filled with healing agent an enclosed air bubble could be identified. When no air bubble can be identified, classifying a capsule as filled is much more difficult due to the limited difference in grey level of air and WRA. Using this method, each capsule was classified as empty or filled with healing agent and it was also established whether it was crossed by the crack or not. The 3D distribution of the capsules in the cores is shown in Fig. 10B. The empty capsules that were crossed by the crack are depicted in red while the other capsules are illustrated in blue.

It can be seen that substantially more glass capsules are dispersed in the concrete core compared to the PMMA capsules (39 versus 19 capsules, respectively). Since the PMMA capsules showed a high survival ratio towards mixing it is unlikely that the lower amount of PMMA capsules present in the core compared to glass is due to breakage during concrete preparation. It is hypothesized that this is rather due to the tendency of the PMMA capsules to float, which resulted in a less homogeneous distribution of the capsules in the beam. One would expect that if the capsules float that they would be more concentrated in one layer. Although, the scanned core covered the complete height of the beam, this was not visible. An explanation can be that during concrete pouring the PMMA capsules were also floating towards the ends of the beams and the μCT analysis was performed on a core drilled away from the edges of the beam (i.e. crack 4 (see Fig. 2)).

3.4.3. Resistance of the self-healed concrete against chloride ingress

The experimentally determined chloride profiles for all cracked and healed samples in the vicinity of the exposed surface are shown in Fig. 11. It can be seen that for three of the healed samples (Glass 1, PMMA 1 and PMMA 2), the chloride concentration is approximately constant at every depth. When comparing with cracked concrete it is clear that the chloride content is considerably reduced due to release of healing agent from the capsules. Next, a similar chloride profile as those of the reference samples was observed for one of the samples containing glass capsules (glass 2). This means that most likely no healing agent was released from the capsules in the considered measuring zone.

The chloride profiles obtained at the crack surface are presented in Fig. 12. First, a more detailed investigation of the chloride profiles per group of samples (REF, Glass or PMMA) is presented.

For the reference samples, the highest chloride concentrations at every depth are found in the zone A. Since this section was ground right next to the exposed surface, the chlorides penetrated through and perpendicular to the crack. This can also explain the fluctuation in the chloride contents observed in this zone. It can also be noticed that for REF 2 a higher chloride concentration was found for a zone deeper inside the crack (i.e. area C) than an area close to the exposure surface (i.e. area B). This is probably due to the presence of microcracks parallel to the crack surface. These microcracks increase the interconnectivity between pores and thus can increase the penetration of chlorides in areas located more distant from the exposure surface.

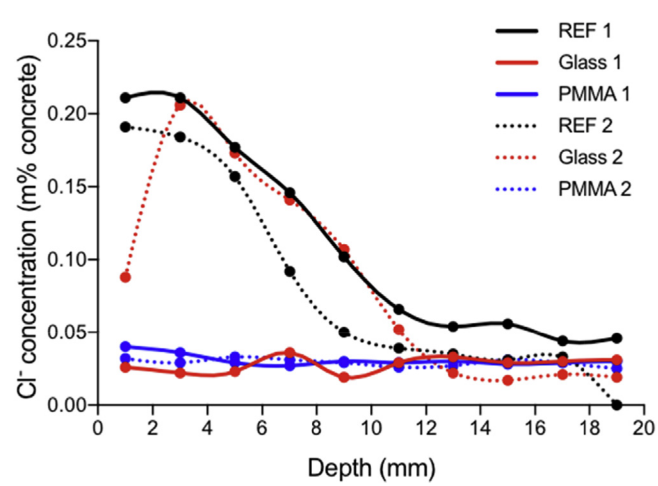

Fig. 11. Chloride profiles in the vicinity of the exposed surface (zone T) obtained after 24 h exposure to a 3 wt% NaCl solution for a time span of 6 weeks.

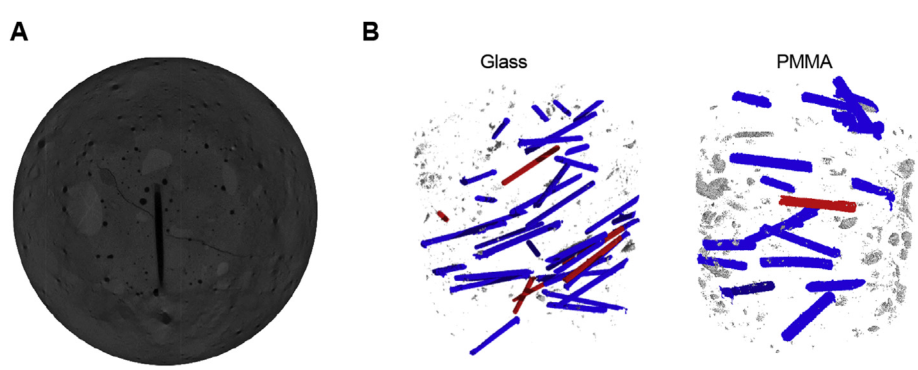

Fig. 10. Reconstructed CT of a sample with a glass capsule crossed by a crack (A); Rendered 3D image of the concrete cores with dispersed capsules (B).

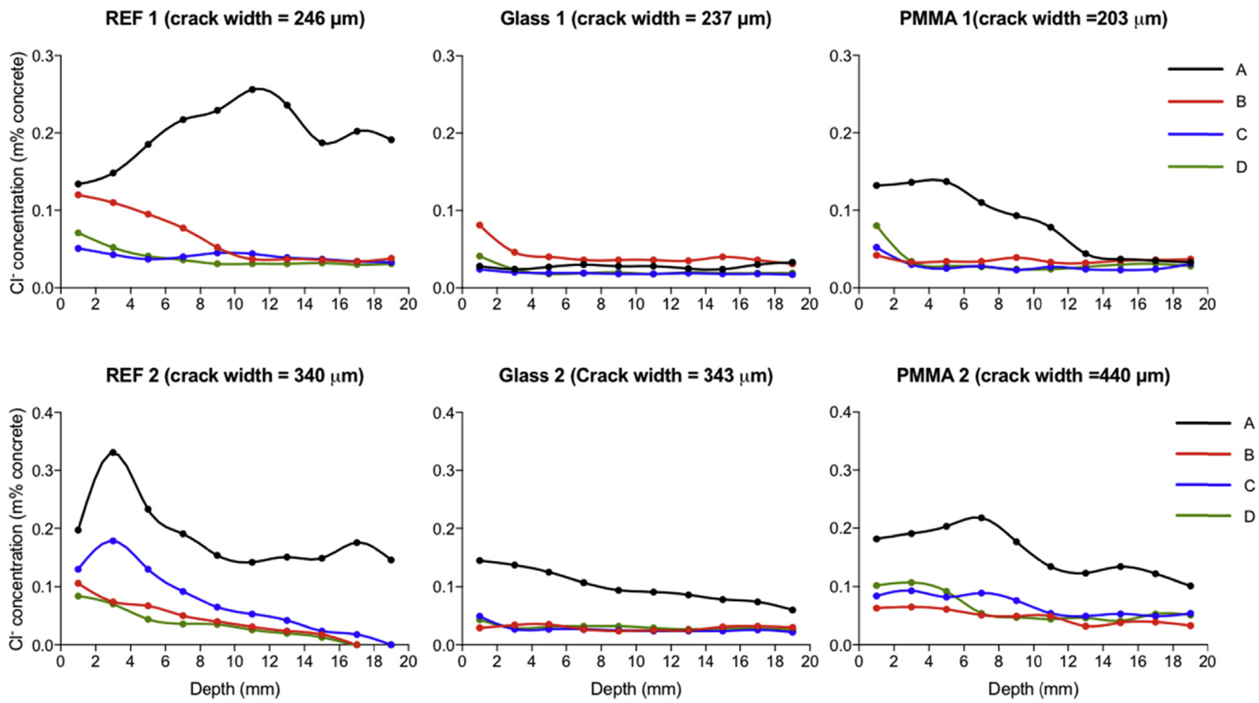

Fig. 12. Chloride profiles in the cracked surface obtained after 24 h exposure to a 3 wt% NaCl solution for a time span of 6 weeks.

The chloride ingress in the samples containing glass capsules is approximately constant, regardless the layer depth (from 4 mm onwards) and the distance from the exposure surface, except for zone A in Glass 2. In this sample, a considerably higher chloride content was measured at the position A. Visual investigation of the spread region of the water-repellent agent (which gives a darker grey color) on the crack face from where material was ground revealed that in this particular section no healing agent was seen, which could explain the higher chloride concentration (Fig. 13).

For the specimens containing PMMA capsules, PMMA 1 showed a chloride profile very similar to the glass 1 profile for sections B, C and D. The chloride concentration in area A is considerably higher since this zone comprised a zone without WRA. Relatively high chloride contents with similar magnitude of the reference samples were found for PMMA 2. Although, the crack width in this sample is slightly higher, the insufficient resistance against chloride penetration is mostly due to falling short of the healing mechanism as visual inspection of the specimen showed that only one capsule released its content.

Overall, it can be seen that the chloride penetration is substantially lower in self-healed samples compared to cracked reference concrete. However, the difference in chloride penetration between cracked reference concrete and concrete containing PMMA capsules was less pronounced, with one of the specimens showing low resistance to chloride ingress.

These results show that the ingress of chlorides is considerably reduced in areas where healing agent was released from the capsules. This stresses the importance of having a uniform distribution of the capsules to achieve higher sealing efficiencies.

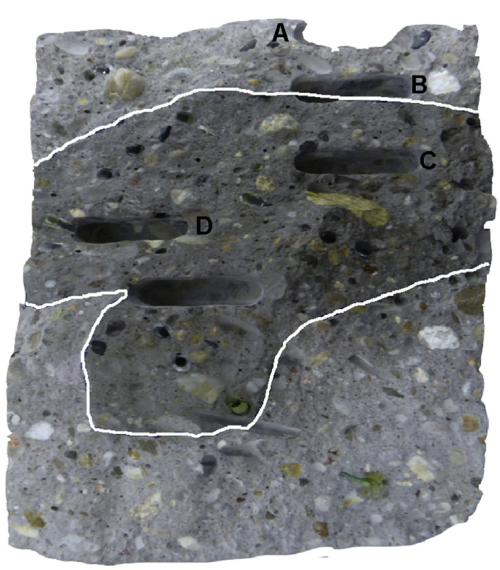

Fig. 13. Split cracked plane of a concrete core (Glass 2), with indication of the ground surfaces. White line indicates the area spread with WRA.

3.4.4. Alkali-silica reaction

Since glass capsules might induce alkali-silica reaction, the resistance of the concrete containing glass capsules to the alkali-silica reaction was determined. Based on literature [35,36], an expansion less than 0.1% was defined as the limit to consider the glass capsules as non-reactive. Moreover, if the expansion values are within the range of 0.1–0.2%, further analysis is required and if the 0.2% value is exceeded, the concrete is considered alkali-silica reactive.

The evolution of the expansion in function of time of concrete samples containing glass capsules is shown in Fig. 14. The limit values (i.e. <0.1%: not reactive (green zone); 0.1–0.2%: undefined and >0.2%: reactive) are also indicated. As can been seen, the expansion exceeded the 0.1% limit after 6 days. Since the expansion is significantly higher than 0.2% after 7 days, the reactivity of the glass capsules with concrete is confirmed.

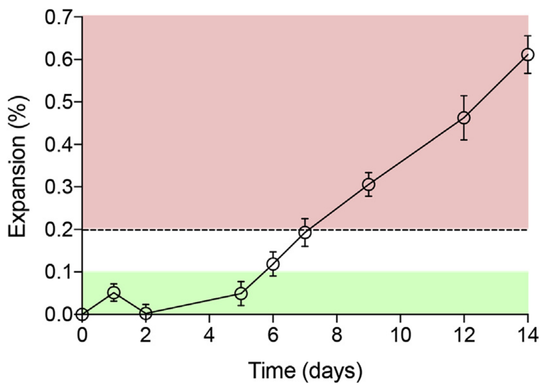

Fig. 14. Evolution of the average expansion of the concrete cylinders containing glass capsules, exposed to a 1 M NaOH solution at 80 °C for 14 days. The error bars represent the standard error (n = 6).

4. Conclusions

The present work has evaluated whether or not polymeric capsules constituted of PMMA can be used to introduce self-healing properties in concrete. The fitness of the PMMA capsules was assessed by determining their robustness during concrete mixing and their probability for breakage to occur upon intersection by a crack in concrete. However, it is necessary to apply a surface treatment to the capsules to induce rupture for relatively small crack widths in concrete (~100 μm). The combined outcome from these experimental tests revealed that PMMA capsules with a wall thickness of approximately 0.7 mm and an outer diameter of about 6.5 mm are the most promising capsules to apply at larger scale.

As alternative to the method of counting manually the number of capsules intact after mixing, a more straightforward method to determine the capsules survival probability during concrete preparation was successfully developed. In this novel method, the setting properties of concrete with encapsulated set accelerator were compared with a calibration curve of setting times in function of set accelerator content.

Real-scale tests revealed that the resistance of cracked concrete against chloride could be increased for concrete made with self-healing properties. In these tests, glass capsules performed better compared to PMMA as a result of a more uniform distribution of the capsules. However, expansion results (Oberholster test) showed that the concrete containing glass capsules is susceptible towards the alkali-silica reaction.

In summary, polymeric capsules constituted of poly(methyl methacrylate) seem to be a promising alternative for the glass capsules that have been used in proof-of-concept experiments to encapsulate healing agent for self-healing concrete. However, future work should be performed to improve the distribution of PMMA capsules in concrete in order to achieve higher healing efficiencies.

Acknowledgments

This research was carried out within the M-ERA.net project “Encapsulation of polymeric healing agents in self-healing concrete: capsule design”, funded by VLAIO (Flanders Innovation & Entrepreneurship) and DGO6 (Walloon Direction Générale Opérationnelle de l'Économie, de l'Emploi et de la Recherche) Project number: 120737. The authors would like to acknowledge these foundations for financial support.

At the time when the experiments were performed, Kim Van Tittelboom was a postdoctoral fellow of the Research Foundation – Flanders (FWO) (project number 12A3314N) and she acknowledges its support.

References

[1] E. Cailleux, V. Pollet, Investigations on the development of self-healing properties in protective coatings for concrete and repair mortars, in: 2nd International Conference on Self-healing Materials, 2009. Chicago.
[2] Z. Yang, J. Hollar, X. He, X. Shi, A self-healing cementitious composite using oil core/silica gel shell microcapsules, Cement Concr. Compos. 33 (4) (2011) 506–512.
[3] M. Pelletier, R. Brown, A. Shukla, A. Bose, Selfhealing Concrete with a Micro-encapsulated Healing Agent, 2011.
[4] B. Dong, G. Fang, W. Ding, Y. Liu, J. Zhang, N. Han, F. Xing, Self-healing features in cementitious material with urea–formaldehyde/epoxy microcapsules, Construct. Build. Mater. 106 (2016) 608–617.
[5] J. Gilford, M.M. Hassan, T. Rupnow, M. Barbato, A. Okeil, S. Asadi, Dicyclopentadiene and sodium silicate microencapsulation for self-healing of concrete, J. Mater. Civ. Eng. 26 (5) (2014) 886–896.
[6] N.P.B. Tan, L.H. Keung, W.H. Choi, W.C. Lam, H.N. Leung, Silica-based self-healing microcapsules for self-repair in concrete, J. Appl. Polym. Sci. 133 (12) (2016) n/a-n/a.
[7] X. Wang, P. Sun, N. Han, F. Xing, Experimental study on mechanical properties and porosity of organic microcapsules based self-healing cementitious composite, Materials 10 (1) (2017).
[8] W. Li, X. Zhu, N. Zhao, Z. Jiang, Preparation and properties of melamine urea-formaldehyde microcapsules for self-healing of cementitious materials, Materials 9 (3) (2016) 152.
[9] E. Gruyaert, K. Van Tittelboom, J. Sucaet, J. Anrijs, S. Van Vlierberghe, P. Dubruel, B.G. De Geest, J.P. Remon, N. De Belie, Capsules with evolving brittleness to resist the preparation of self-healing concrete, 66, 2016, 323.
[10] B. Hilloulin, K. Van Tittelboom, E. Gruyaert, N. De Belie, A. Loukili, Design of polymeric capsules for self-healing concrete, Cement Concr. Compos. 55 (2015) 298–307.
[11] C.M. Dry, Three designs for the internal release of sealants, adhesives, and waterproofing chemicals into concrete to reduce permeability, Cement Concr. Res. 30 (12) (2000) 1969–1977.
[12] R. Lark, C. Joseph, B. Isaacs, D. Gardner, A. Jefferson, Experimental Investigation of Adhesive-based Self-healing of Cementitious Materials, vol 62, 2010.
[13] J. Wang, K. Van Tittelboom, N. De Belie, W. Verstraete, Use of silica gel or polyurethane immobilized bacteria for self-healing concrete, Construct. Build. Mater. 26 (1) (2012) 532–540.
[14] K. Van Tittelboom, N. De Belie, D. Van Loo, P. Jacobs, Self-healing efficiency of cementitious materials containing tubular capsules filled with healing agent, Cement Concr. Compos. 33 (4) (2011) 497–505.
[15] V.C. Li, Y.M. Lim, Y.-W. Chan, Feasibility study of a passive smart self-healing cementitious composite, Compos. B Eng. 29 (6) (1998) 819–827.
[16] J.W.C. Pang, I.P. Bond, A hollow fibre reinforced polymer composite encompassing self-healing and enhanced damage visibility, Compos. Sci. Technol. 65 (11) (2005) 1791–1799.
[17] S. Sangadji, H.E.J.G. Schlangen, Porous Network Concrete: a New Approach to Make Concrete Structures Self-healing Using Prefabricated Porous Layer (Abstract), 2011.
[18] P. Minnebo, G. Thierens, G. De Valck, K. Van Tittelboom, N. De Belie, D. Van Hemelrijck, E. Tsangouri, A novel design of autonomously healed concrete: towards a vascular healing network, Materials 10 (1) (2017).
[19] C. Litina, A. Kanellopoulos, A. Al-Tabbaa, Alternative repair system for concrete using microencapsulated healing agents, in: Concrete Solutions: Proceedings of Concrete Solutions, 5th International Conference on Concrete Repair, 2014, pp. 97–103.
[20] L. Lv, E. Schlangen, Z. Yang, F. Xing, Micromechanical properties of a new polymeric microcapsule for self-healing cementitious materials, Materials 9 (12) (2016).
[21] K. Van Tittelboom, N. De Belie, Self-healing in cementitious materials—a review, Materials 6 (6) (2013) 2182–2217.
[22] K. Van Tittelboom, E. Tsangouri, D. Van Hemelrijck, N. De Belie, The efficiency of self-healing concrete using alternative manufacturing procedures and more realistic crack patterns, Cement Concr. Compos. 57 (2015) 142–152.
[23] J. Feiteira, E. Gruyaert, N. De Belie, Self-healing of moving cracks in concrete by means of encapsulated polymer precursors, Construct. Build. Mater. 102 (2016) 671–678.
[24] J. Feiteira, Self-healing Concrete Encapsulated Polymer Precursors as Healing Agents for Active Cracks, Doctoral dissertation, University of Ghent, 2017.
[25] B. Šavija, J. Feiteira, M. Araújo, S. Chatrabhuti, J.-M. Raquez, K. Van Tittelboom, E. Gruyaert, N. De Belie, E. Schlangen, Simulation-aided design of tubular polymeric capsules for self-healing concrete, Materials 10 (1) (2017) 10.
[26] N. Robeyst, E. Gruyaert, C.U. Grosse, N. De Belie, Monitoring the setting of concrete containing blast-furnace slag by measuring the ultrasonic p-wave velocity, Cement Concr. Res. 38 (10) (2008) 1169–1176.
[27] M. Araújo, S. Van Vlierberghe, J. Feiteira, G.-J. Graulus, K. Van Tittelboom, J.C. Martins, P. Dubruel, N. De Belie, Cross-linkable polyethers as healing/sealing agents for self-healing of cementitious materials, Mater. Des. 98 (2016) 215–222.

[28] M. Song, Chloride Penetration and Service Life Prediction of Cracked Self-compacting Concrete, 2012. PhD thesis. Ghent.
[29] V. Cnudde, M.N. Boone, High-resolution X-ray computed tomography in geosciences: a review of the current technology and applications, Earth Sci. Rev. 123 (Supplement C) (2013) 1–17.
[30] M. Bert, D. Manuel, L. Denis Van, N.B. Matthieu, B. Loes, P. Elin, C. Veerle, H. Luc Van, HECTOR: a 240kV micro-CT setup optimized for research, J. Phys. Conf. 463 (1) (2013), 012012.
[31] J. Vlassenbroeck, M. Dierick, B. Masschaele, V. Cnudde, L. Van Hoorebeke, P. Jacobs, Software tools for quantification of X-ray microtomography at the UGCT, Nucl. Instrum. Methods Phys. Res. Sect. A Accel. Spectrom. Detect. Assoc. Equip. 580 (1) (2007) 442–445.
[32] L. Brabant, J. Vlassenbroeck, Y. De Witte, V. Cnudde, M.N. Boone, J. Dewanckele, L. Van Hoorebeke, Three-dimensional analysis of high-resolution X-ray computed tomography data with Morpho+, Microsc. Microanal. 17 (2) (2011) 252–263.
[33] N. De Belie, C.U. Grosse, J. Kurz, H.W. Reinhardt, Ultrasound monitoring of the influence of different accelerating admixtures and cement types for shotcrete on setting and hardening behaviour, Cement Concr. Res. 35 (11) (2005) 2087–2094.
[34] T.D.P. Thao, T.J.S. Johnson, Q.S. Tong, P.S. Dai, Implementation of self-healing in concrete – proof of concept, IES J. Part A Civ. Struct. Eng. 2 (2) (2009) 116–125.
[35] J.PG. Desmyter, P. Demars, J. Jacobs, De alkali-silica reactie, WTCB Tijdschrift 3–17.
[36] E. Gruyaert, M. Maes, N. De Belie, Performance of BFS concrete: k-Value concept versus equivalent performance concept, Construct. Build. Mater. 47 (Supplement C) (2013) 441–455.